15. CLAY AND ASSOCIATED MINERALS IN SEDIMENTS FROM THE NAURU BASIN, DEEP SEA DRILLING PROJECT LEG 61[1]

V. B. Kurnosov, Far-East Geological Institute of the Far-East Science Center of the U.S.S.R. Academy of Sciences, Vladivostok, U.S.S.R.
and
A. Ya. Shevchenko, Institute of Oceanology, Moscow, U.S.S.R.

INTRODUCTION

Three units of Cenomanian–Pleistocene sediments were drilled at Site 462: from 0 to 297 meters Oligocene–Pleistocene calcareous and radiolarian oozes and chalk, mainly of turibiditic nature; from 297 to 447 meters Maestrichtian–Eocene chert, chalk, and limestones; from 447 to 599 meters, Cenomanian–Maestrichtian volcaniclastic sandstones, claystones, and limestones. In middle Cretaceous basalts, hyaloclastic sediments are found (Unit IV); in the interval from 560 to 730 meters, they are intercalated with sills. In the other part of the volcanogenic complex, from 730 to 1068 meters, one sedimentary interbed has been found, at a depth of 992 meters.

Sixty samples from sediments of Nauru Basin have been studied mineralogically in the <2-μm, 2 to 20-μm, and >20-μm fractions, and in bulk. Identification of minerals is based on X-ray-diffraction analysis, electron-diffraction analysis, infrared spectral analysis, electron-microscopy data, scanning-electron-microscopy data, wet chemical analysis, and spectral analysis of minor elements. Methods of identification of clay and associated minerals are described in detail in Kurnosov et al. (1980).

MINERALS AND THEIR CHEMICAL COMPOSITION

Swelling minerals, hydromica, chlorite, kaolinite, mixed-layer chlorite–montmorillonite, palygorskite, sepiolite, clinoptilolite, heulandite–clinoptilolite, cristobalite–tridymite (opal-CT), quartz, feldspar, calcite, analcime–wairakite, actinolite–tremolite, talc, and amorphous phases are identified in sediments from the Nauru Basin.

Dioctahedral and trioctahedral smectite and mixed-layer hydromica–montmorillonite belong to 17 Å minerals.

Dioctahedral Fe-smectite (Fe-montmorillonite) has a *b* parameter of 9.04 to 9.09 Å (Table 1). X-ray data and infrared (IR) spectra are normal. A chemical analysis is presented in Table 2. Electron micrographs of Fe-montmorillonite, studied in Samples 462-48-2, 75–77 cm; 462-49-3, 1–4 cm; 462-57,CC; 462A-9-3, 58–61 cm; and 462-11-1, 60–64 cm usually show a cloud-like shape (Plate 1, Figs. 1, 2, and 3). Besides, they sometimes show plate-like transparent lamellae (Plate 1, Fig. 2), which probably belong to needle-like and plate-like smectites (Kossovskaya and Shutov, 1975; Butuzova et al., 1979). Besides the usual lacy Fe-montmorillonite, which has replaced volcanic glass (Plate 2, Figs. 1 and 2), rounded Fe-montmorillonites of crimp structure (Sample 462-48-2, 75–77 cm; Plate 3, Fig. 1) and columnar ones with a lacy surface (Sample 462-57,CC; Plate 3, Fig. 1) are discovered by the SEM.

Table 1. The *b* parameter of smectites from Leg 61 sediments.

Sample (interval in cm)	Sub-bottom Depth (m)	*b* Parameter (Å)
462-1-2, 136–140	3.0	9.07, 9.21
5-2, 68–72	40.5	9.05, 9.25
8-4, 95–99	72.0	9.05
12-4, 8–12	109.5	9.02, 9.20
18-3, 74–78	165.5	9.05
36-4, 54–57	338.0	9.05
38-1, 106–109	353.0	9.05
48-2, 75–77	449.0	9.06
49-1, 103–106	457.5	9.09
49-3, 1–4	459.5	9.07
50-2, 138–141	468.5	9.07, 9.20
56-1, 147–158	523.5	9.09
57,CC	540.5	9.07
59-1, 0–5	549.5	9.04
462A-9-3, 6–11	518.5	9.05
9-3, 58–61	519.0	9.05
10-2, 109–116	528.0	9.04
11-1, 60–68	535.0	9.04
12-1, 75–78	544.5	9.05
13-1, 110–113	554.5	9.05

Trioctahedral smectite (Fe–Mg-saponite) has a *b* parameter of 9.19 to 9.25 Å (Table 3). According to Mering (1975), saponite belongs to semi-ordered type II. Chemical analyses of saponites with a small impurity of other minerals are presented in Table 4. The saponites contain less SiO_2 and more FeO and MgO than Fe-montmorillonites.

Electron micrographs of saponites show the usual cloud-like shape, and scanning electron micrographs show a petalous texture (Plate 2, Figs. 3, and 4), as well as plate- and needle-like textures.

[1] *Initial Reports of the Deep Sea Drilling Project*, Volume 61.

Table 2. Wet chemical analysis of the <2-μm fraction of Leg 61 sediments.

Component	Sample 462-8-4, 95–99 cm*	462-48-2, 75–77 cm*	462-57-1, 68–71 cm*	462-60-1, 40–42 cm*	462A-9-3, 58–61 cm*	462A-10-2, 109–116 cm	462A-11-1, 60–64 cm*	462A-14-1, 85–88 cm*
SiO_2	49.20	50.30	52.60	53.10	40.60	52.60	49.80	56.90
TiO_2	1.47	2.06	1.12	0.42	1.46	0.77	1.31	0.45
Al_2O_3	5.43	10.21	14.58	8.05	9.94	14.85	14.59	8.09
Fe_2O_3	21.09	8.60	8.03	13.94	9.38	9.33	11.32	8.07
FeO	0.41	0.41	0.41	0.48	0.34	0.27	0.34	1.03
MnO	0.24	0.08	0.10	1.70	0.12	0.18	0.12	2.60
MgO	9.48	5.97	3.35	2.25	4.28	3.81	3.76	3.61
CaO	0.00	3.05	1.60	1.21	11.97	2.41	1.12	0.96
Na_2O	0.40	0.68	0.38	0.22	0.38	0.32	0.57	0.24
K_2O	0.97	0.29	1.05	2.02	1.05	2.45	1.26	1.79
L.o.i.	7.88	10.90	9.32	10.51	15.38	8.00	10.59	8.71
H_2O^-	3.75	7.04	7.70	6.02	5.05	5.45	5.00	7.23
Total	100.32	99.59	100.24	99.92	99.95	100.41	99.78	99.68

*Fe-montmorillonite predominates in the <2-μm fraction.

Table 3. The *b* parameter of smectites from volcaniclastic sediments in basalt, Leg 61.

Sample (interval in cm)	Sub-bottom Depth (m)	*b* (Å)	Type of Stacking of Smectite Layers*
462-64-1, 40–42	585.5	9.21	II
64-2, 35–38	587.0	9.23	II
64-3, 20–24	588.5	9.23	II
65-1, 6–8	594.5	9.19	II
462A-22-2, 88–90	590.0	9.24	II
23-1, 0–2	597.0	9.24	II
40-1, 140–142	703.0	9.24	II
42-2, 95–97	722.5	9.23	II
79-6, 4–6	992.5	9.25	II
80-1, 18–21	994.0	9.25	II
80-1, 34–36	994.0	9.25	II
80-2, 25–28	995.5	9.23	II
80-2, 97–102	996.0	9.22	II

* II = semi-ordered stacking (Mering, 1975)

Mixed-layer, disordered hydromica–montmorillonite is identified in X-ray-diffraction patterns by the asymmetric and broad 17 Å reflection (Dritz and Sakharov, 1976). The ratio of 17 Å peak heights (*Z*) of the mixed-layer mineral averages 0.5, whereas that of Fe-montmorillonite is 0.8 to 0.9 (Table 5). The shape of the mixed-layer mineral is the same as that of Fe-montmorillonite, that is, cloud-like (Plate 1, Fig. 5).

Hydromica is dioctahedral, of 1M and 2M, polytypes. Chlorite is trioctahedral, ferromagnesian, well crystallized, it also may be imperfect, with a hydrated brucite layer. Kaolinite is scarcely identifiable in Sample 462-12-4, 8–12 cm by its IR spectrum. Mixed-layer chlorite–montmorillonite is identified by weak reflections at 11.8 to 12.8 Å, after heating at 500°C/hr.

Palygorskite–sepiolite are identified in X-ray and electron-diffraction patterns mainly by 10.4–10.5 Å and 11.8 Å reflections and are prominent on electron photomicrographs (Plate 1, Fig. 6; Plate 4, Figs. 1, 2).

Talc is identified in X-ray-diffraction patterns by 9.3 to 9.4-Å reflections, but this identification is often indefinite, because the reflection is weak (Table 5).

Clinoptilolite, heulandite–clinoptilolite, cristobalite–tridymite, quartz, calcite, analcime–wairakite, actinolite–tremolite, feldspar, and amorphous phases are identified by X-ray (Kurnosov et al., this volume). Plates 5 to 7 show the morphology of secondary minerals.

Chemical composition and minor elements were studied in the <2-μm fraction of sediments from the Nauru Basin. The results are presented in Tables 2, 4, 6, and 7.

DISTRIBUTION OF CLAY AND ASSOCIATED MINERALS IN SEDIMENTS

Units I and II

In sediments of Units I and II, pelagic clays include mixed-layer hydromica–montmorillonite, hydromica of $2M_1$ and 1M polytypes, chlorite, and admixtures of kaolinite, mixed-layer chlorite–montmorillonite, quartz,

Table 4. Wet chemical analyses of the <2-μm fraction from volcaniclastic sediments interbedded with basalt, Leg 61.

Component	Sample 462-63-1, 25–27 cm	462-64-1, 40–42 cm	462-64-2, 35–38 cm	462-64-3, 20–24 cm	462-65-1, 6–8 cm	462A-79-6, 4–6 cm	462A-80-2, 25–28 cm	462A-80-2, 97–102 cm
SiO_2	41.52	42.25	40.75	41.45	40.65	43.10	37.20	35.95
TiO_2	0.65	0.77	0.87	0.72	0.69	1.11	1.51	1.46
Al_2O_3	7.66	9.85	11.74	11.40	10.78	11.80	8.48	9.02
Fe_2O_3	11.57	10.80	11.10	9.25	10.20	11.02	13.84	13.76
FeO	2.67	2.74	2.39	3.83	2.97	2.67	1.78	2.05
MnO	0.06	0.11	0.11	0.14	0.14	0.17	0.10	0.12
MgO	10.33	12.83	10.52	12.25	11.10	8.21	11.79	11.68
CaO	2.32	1.45	2.09	1.61	1.61	3.54	2.57	2.09
Na_2O	0.65	0.27	0.24	0.14	0.24	3.08	0.24	0.37
K_2O	0.29	0.96	1.70	1.73	1.64	0.52	0.11	0.16
L.o.i.	14.14	10.93	11.12	10.28	11.64	8.68	15.03	15.24
H_2O^-	8.25	7.19	6.91	7.00	7.89	5.71	7.16	7.81
Total	100.11	100.15	99.54	99.80	99.55	99.61	99.81	99.71

feldspar, and clinoptilolite (Table 5). The composition of this complex of minerals, excluding clinoptilolite, is invariable through the whole Oligocene–Pleistocene section. It is impoverished in calcite and amorphous phases to various degrees. When calcite and (or) amorphous phases prevail in carbonaceous and siliceous sediments, clay minerals often occur as an admixture. We failed to separate the <2-μm fraction from carbonaceous sediments.

Sample 462-8-4, 95–99 cm contradicts the regularity of mineral distribution in Units I and II. The <2-μm fraction from this sample consists of Fe-montmorillonite, with hydromica, palygorskite, clinoptilolite, and cristobalite–tridymite admixtures. Fragments of alkali and tholeiitic basalts were separated from the >20-μm fraction. Altered fragments of tholeiitic basalt are composed of Fe–Mg-saponite. Fragments of alkali glass are fresh. Fresh fragments of alkali glass also occur in Sample 462-15-1, 44–47 cm.

Unit III

The mineral complex of volcaniclastic sediments of Unit III differs in composition from those of Units I and II. The main differences are as follows. In sediments of Unit III Fe-montmorillonite prevails among clay minerals; kaolinite and trioctahedral minerals (chlorite and mixed-layer chlorite–montmorillonite) are practically lacking. Some layers are rich in palygorskite. Volcaniclastic sediments contain much clinoptilolite. In the lower part of the unit, at the contact with basalt, there is a large amount of siliceous minerals: quartz and cristobalite–tridymite (Table 5).

In these sediments, red and pinkish clays (Samples 462-56-1, 147–158 cm; 462-59-1, 0–5 cm; 462A-10-2, 109–116 cm; 462A-12-1, 75–78 cm; 462A-13-1, 110–113 cm) are polymineralic and comprise much palygorskite, as well as mixed-layer hydromica–montmorillonite and $2M_1$ and 1M hydromica. Sometimes red clays contain chlorite and kaolinite admixtures. Dark-brown clays and argillites (Samples 462-57-1, 68–71 cm; 462-58-4, 6–10 cm; 462A-11-1, 60–64 cm) interbanded with red clays either do not contain palygorskite or contain very little. In the <2-μm fraction, Fe-montmorillonite prevails (Table 5). In the 2- to 20-μm and >20-μm fractions, mixed-layer hydromica–montmorillonite contains less hydromica packets than the mixed-layer mineral from red clays.

The mineralogical composition of volcaniclastic sandstones (Hole 462, Cores 48–51, 57; 462A-7-1, 46–51 cm) and argillite at the contact with basalt (Sample 462A-14-1, 85–88 cm) is like that of the dark-brown clays. Fe-montmorillonite is a primary clay mineral in sandstone. The 2- to 20-μm and >20-μm fractions comprise mixed-layer hydromica–montmorillonite, hydromica, and chlorite, with kaolinite.

Clinoptilolite occurs in sediments of all types, although it is most common in clays and argillites and is concentrated in the 2- to 20-μm and >20-μm fractions (Table 5). In the lower part of Unit III clinoptilolite is lacking in sediments at the contact with basalt. Feldspar is observed in almost all samples. The largest quantity of quartz is found in sediments about 10-meters thick near the contact. Above this, quartz is replaced by cristobalite–tridymite. Calcite is found in large quantities in the uppermost sediments of Unit III, down to 519 meters. Small quantities of sepiolite are identified by electron-diffraction analysis in Samples 462-49-1, 103–106 cm; 462-50-2, 138–141 cm. Sepiolite occurs with palygorskite.

Two fragments of sandstones of the upper part of Unit III (Sample 462-48-2, 75–77 cm) were analyzed. A fragment of white siliceous rock is composed of calcite, cristobalite–tridymite, clinoptilolite, and admixtures of quartz and 17-Å mineral. A green fragment of altered volcanic glass consists mainly of Fe-montmorillonite, feldspar, and amorphous phases, with a broad reflection near 4.45 Å, typical of palagonite.

Unit IV

Twenty-four samples from volcaniclastic interbeds of the Nauru Basin sill complex were analyzed. The mineralogy of these samples was studied in bulk. Other samples were studied in <2-μm, 2- to 20-μm, and >20-μm fractions (Table 8). The mineralogical composition of volcaniclastic sediments from the sill complex is peculiar and differs sharply from sediments overlying basalts, including volcaniclastic sediments of Unit III (Table 8).

In all samples analyzed in bulk and in fractions, Fe–Mg-saponite is the principal mineral. Other minerals (hydromica, chlorite, analcime–wairakite, heulandite–clinoptilolite, actinolite–tremolite, and talc) occur as admixtures. Among admixture minerals, analcime–wairakite is most common, chlorite and actinolite–tremolite are also widespread. Heulandite–clinoptilolite is identified in that part of the section in which the participants of Leg 61 found zeolite veinlets in sediments. Talc is found in the lowermost sedimentary interbeds between thick sills (Table 8).

The chemical composition of volcaniclastic sediments overlying basalt and within basalts is compared in the <2-μm fraction (Tables 2 and 4); the results are presented in a triangular diagram for the <2-μm fraction composition, involving Fe_2O_3 + FeO, Al_2O_3, and MgO (Fig. 1), and in a rectangular diagram of (Fe_2O_3 + FeO + MgO)/Al_2O_3 and Na_2O + K_2O (Fig. 2). The diagrams show that sediments interbedded with basalt contain more magnesium and less Al_2O_3 than sediments overlying the sill complex. Two samples (462-8-4, 95–99 cm, from a volcaniclastic interbed in terrigenous sediment of Unit I; 462-60-1, 40–42 cm, from a near-contact layer) are exceptions. They are enriched in Fe_2O_3 (Table 2).

The total alkalies in volcaniclastic sediments of Units III and IV are identical (Fig. 2). Only in the lowermost sedimentary interbed in basalt, at a depth of 992 meters, is the alkali content in Core 80 decreased, and in Core 79 is the lowest Na_2O content, 3.08% (Table 4).

Sediments overlying basalts contain more SiO_2 than sediments within basalts (Tables 2 and 4).

In sediments overlying basalt, with the approach to the contact SiO_2, MnO, K_2O, Fe_2O_3 + FeO (Hole 462), and FeO (Hole 462A) increase, whereas TiO_2, Al_2O_3,

Table 5. Clay-mineral compositions and fractions of related minerals (%): <2 μm (1), 2–20 μm (2), and >20 μm (3), Site 462.

Sample (interval in cm)	Sub-bottom Depth (m)	Lithology	Age	17-Å Minerals			Hydromica			Chlorite + Kaolinite			Mixed-Layer Chlorite-Montmorillonite		
				1	2	3	1	2	3	1	2	3	1	2	3
462-1-1, 22–26	0.5	Unit 1: calcareous	Pleistocene		30			50			20				
1-2, 136–140	3.0	and radiolarian oozes		47	45		32	30		21	25		tr	tr	
3-5, 16–19	25.5	and chalks		75			15			10			tr		
4-4, 48–50	33.5				75	tr		15			10				
4-5, 116–128	36.0				70			15			15			tr	
5-2, 68–72	40.5			75	65		15	20		10	15		tr	tr	
6-4, 91–95	53.0			78	80	tr	11	15		11	5		tr	tr	
8-4, 95–99	72.0			100	85	tr	tr	10	tr		5			tr	
10-3, 62–65	89.5		Middle	60	70	tr	30	20	tr	10	10	tr		tr	
11-3, 138–142	99.5		Miocene	65	65		18	20		17	15		tr	tr	
12-4, 8–12	109.5			70	60		20	30		10	10		tr	tr	
13-1, 58–62	115.0				tr										
14-6, 65–67	132.0		Early	60	60	tr	25	20	tr	15	20	tr	tr	tr	
15-1, 44–47	143.0		Miocene		60	tr		20	tr		20	tr		tr	
17-2, 109–113	155.0		Late		90			10			tr			tr	
18-3, 74–78	165.5		Oligocene	90	90		7	5		3	5			tr	
19-4, 114–118	176.5			70	75	75	25	15	10	5	10	15	tr	tr	
20-4, 83–87	186.0				90			10							
24-4, 65–68	224.0			tr	100		tr			tr					
25-3, 92–95	232.0				tr										
27-3, 84–87	251.0		Early		tr										
28-6, 102–108	265.5		Oligocene		tr										
36-4, 54–57	338.0	Unit 2: cherts, chalks,	Eocene	75	75	tr	15	15		10	10		tr	tr	
38-1, 106–109	353.0	and limestones		80	65		15	20		5	15		tr	tr	
39-2, 100–104	364.0			75	75		20	20		5	5				
462A-7-1, 46–51	439.5		Maestrichtian	100	100	tr									
48-2, 75–77	449.0	Unit 3: volcaniclastic		100	100	100									
462-49-1, 103–106	457.5	sediments, zeolitic		100											
49-3, 1–4	459.5	claystones, and		95	85		5	10			5				
50-2, 138–141	468.5	black shales		85	90	100	10	5		5	5				
51-2, 55–63	477.5					95			5						
462A-9-3, 6–11	518.5		Early	70			30								
9-3, 58–61	519.0		Campanian	100	100	100	tr	tr							
462-56-1, 147–158	523.5		?	50	35		30	52		2	3				
462A-10-2, 109–116	528.0			60	40	40	18	40	35	2	5	2			
462-57-1, 68–71	532.0		Early	100	100		tr								
462A-11-1, 60–64	535.0		Santonian	100	100	90	tr		10						
462-57,CC	540.5			100	100	100									
58-2, 32–35	542.0		Early	tr			tr								
462A-12-1, 75–78	544.5		Santonian–		55			25							
462-58-4, 6–10	545.0		Late Turonian	100	95	90		5	10						
59-1, 0–5	549.5		Cenomanian	tr	tr	90	tr	tr	tr						
462A-13-1, 110–113	554.5			tr	tr	40	85	85	40						
462-60-1, 40–42	558.5			80	80	90	20	20	10						
462A-14-1, 85–88	563.5			100	75	75		20	20		5	5			

+ + = abundant, + = common, tr = trace.

Fe_2O_3 (Hole 462A), MgO, CaO, and Na_2O decrease (Table 2). Cr, Ni, Co, Sc, Pb, and especially Cu contents increase in sediments with the approach to the contact with basalts. This peculiarity in minor-element distribution is prominent in Hole 462A and is lacking in Hole 462 (Table 6).

GENESIS OF MINERALS

Units I and II

In Eocene–Pleistocene time, calcareous and siliceous sediments accumulated in Nauru Basin; clay minerals were primarily terrigenous. A complex of clay minerals typical of terrigenous sediments of the Pacific equatorial sector on the whole is found in interbeds of pelagic clays (Griffin et al., 1968). This complex consists of mixed-layer hydromica–montmorillonite, $2M_1$ and 1M hydromica, chlorite, and an admixture of kaolinite and mixed-layer chlorite–montmorillonite, quartz, feldspar, and amorphous phases.

The background accumulation of pelagic clays was restrained to various degrees by active calcareous accumulation. Sediments with calcite were introduced by suspension flows from the slopes of the Marshall Islands and Caroline Islands, surrounding Nauru Basin (data of participants of Leg 61). The composition of the clay-mineral complex in the calcareous and carbonaceous sediments is the same as in the pelagic clays.

Thus, from the Eocene to the Recent, homogeneous clay material was introduced into Nauru Basin. Streams which transported it were stable in that period. Accumulation of silica prevailed in the Eocene and continued

Table 5. (Continued).

	Z		Palygorskite–Sepiolite			Quartz			Feldspar			Clinoptilolite			Cristobalite–Tridymite			Calcite			Amorphous Phases		
1	2	3	1	2	3	1	2	3	1	2	3	1	2	3	1	2	3	1	2	3	1	2	3
	0.5						+			tr												tr	
0.6	0.4					+	+		tr	+											tr	tr	
0.7						tr			tr												tr		
	0.5	0.5					tr	tr		tr	tr							+ +	+		tr	tr	
	0.6						tr			tr											+	+	
0.6	0.4					tr	tr		tr	tr											+	+	
0.4	0.6	0.5				tr	tr		tr	tr											+	+	+
0.8	0.6		tr				tr	tr	tr	tr	tr	tr			tr			+ +	tr			tr	+ +
0.3	0.3	0.3				tr	tr	tr	tr				tr						tr		+	+	+ +
0.5	0.4					tr	tr		tr	tr			tr								+	+	
0.5	0.5					tr	tr		tr	tr											+	+	
																		+ +	+ +				
0.4	0.4	0.4				tr	tr	tr	tr	tr	tr										+	+	+
	0.5	0.5						tr			tr							+ +	+ +		+		tr
	0.5						tr			tr								tr				+	
0.6	0.5					tr	tr		tr	tr		tr	tr								tr	+	
0.3	0.6	0.3				tr	tr	tr	tr	tr	tr	tr									+	+	+
	0.6									tr			tr					+				tr	
	0.5					tr			tr			+			tr			+ +			+	+	
																		+ +				tr	
																		+ +					
																		+ +	+				+
0.4	0.5	0.3				tr	tr	tr	tr	tr											+	+	+ +
0.4	0.3		tr			tr	tr		tr	tr											+	+	
	0.4					tr			tr												+ +	+ +	
0.9	0.8											tr	+	+				tr	+ +	+ +			
0.9	0.9	0.7								tr								tr	+			tr	tr
0.6			tr									tr			tr			+ +			tr		
0.8	0.7											tr	+ +										
0.8	0.8	0.8	tr						tr	tr								tr				tr	tr
		0.7												tr					+ +				tr
0.8			tr			tr			tr			tr						+ +			tr		
0.9	0.9	0.8	tr							tr				+				+	tr	+			
0.6	0.4		18	10		tr	+		tr	+			+								tr	tr	
0.7	0.4	0.4	20	15	23	tr	+	tr	tr	+	tr	tr	tr	tr								tr	tr
0.9	0.8								tr	tr		tr	tr										
0.8	0.6	0.6	tr				tr	tr	tr	+	tr	tr	+ +	+ +					tr			tr	tr
0.9	0.8	0.6							tr	+	tr		tr	tr					tr			tr	tr
						tr									+ +								
	0.4			15			tr			tr			+ +			tr						tr	
0.8	0.6	0.6						tr		tr	tr		+	+ +	tr	tr	tr					tr	tr
		0.4	tr	tr	10	+	+	+			tr	tr	+	tr	+ +	+	+		tr		tr	tr	tr
		0.4	15	15	20	+ +	+ +	+ +	tr	tr	tr	+	+ +	+			tr				tr	tr	tr
0.2	0.4	0.6				+	+	+ +															
0.9	0.6	0.7					+ +	+ +															

Table 6. Trace elements (ppm) in the <2-μm fraction of Leg 61 sediments.

Sample (interval in cm)	Sub-bottom Depth (m)	Cr	Ni	V	Co	Zr	Sc	Pb	Sn	Cu
462-8-4, 95–99	72.0	100	175	30	40	160	21	5	—	160
48-2, 75–77	449.0	30	61	112	—	89	7	—	—	34
50-2, 138–141	468.5	80	220	65	37	115	15	9	—	25
57-1, 68–71	532.0	40	91	180	14	148	25	6	—	83
59-1, 0–5	549.5	45	70	45	12	150	12	9	—	200
60-1, 40–42	558.5	28	60	83	25	79	19	9	7	300
462A-9-3, 58–61	518.5	39	120	120	25	160	13	11	—	16
10-2, 109–116	528.0	30	75	64	25	107	17	14	—	57
11-1, 60–64	535.0	30	120	120	35	160	19	14	—	57
13-1, 110–113	554.5	43	160	66	63	150	25	19	—	200
14-1, 85–89	563.5	40	105	140	180	120	27	17	3	220

to the late Pleistocene. In the Oligocene–Pleistocene, silica accumulation was accompanied by intensive introduction of carbonates, which often prevailed.

In some layers of Unit I containing volcaniclastic material (Sample 462-8-4, 95–99 cm), Fe-montmorillonite as well as an admixture of palygorskite, clinoptilolite, and cristobalite–tridymite were formed, mainly because of decomposition of volcanic glass. The fragments of tholeiitic basalts with trioctahedral smectite (Fe–Mg-saponite) in the coarse fraction of the volcaniclastic material show that the basalt complex studied in Holes 462 and 462A has undergone erosion. Fragments

Table 7. Trace elements (ppm) in the <2-μm fraction of sediments interbedded with basalt, Leg 61.

Sample (interval in cm)	Sub-bottom Depth (m)	Cr	Ni	V	Co	Zr	Sc	Pb	Sn	Cu
462-64-2, 35-38	587.0	112	87	170	34	65	44	—	—	80
64-3, 20-24	588.5	110	90	150	30	63	50	—	—	73
462A-79-6, 4-6	992.5	60	66	190	25	63	48	5	—	118
80-2, 25-28	995.5	125	120	112	—	57	38	—	—	75
80-2, 97-102	996.0	120	140	180	—	65	40	—	—	46

of slightly altered alkali volcanic glass in Samples 462-8-4, 95-99 cm and 462-15-1, 44-47 cm reflect the activation of island alkali volcanism (Shcheka, this volume).

Diagenetic changes of clay minerals in sediments of Units I and II have not been observed.

Unit III

In Cenomanian-Maestrichtian time, abundant volcaniclastic material was introduced into the Nauru Basin, which determined the mineralogical composition of sediments of Unit III. Alteration of volcanic glass in sandstones and clays caused the formation of Fe-montmorillonite, clinoptilolite, and probably some 1M mica. Residues of palagonitized glass are visible in thin sections of sandstones; they are also visible in X-ray-diffraction patterns by the amorphous background and broad, asymmetric 4.5-Å reflection. This reflection is common in X-ray-diffraction patterns of palagonitized glass in samples from the Pacific and Indian Oceans.

Mixed-layer hydromica-montmorillonite, which represents 17-Å minerals in red clays and in the 2- to 20-μm and >20-μm fractions of brown clays, is probably terrigenous. $2M_1$, and particularly 1M hydromica, as well as chlorite, kaolinite, calcite, amorphous phases, feldspar, and quartz, also are terrigenous. This complex of terrigenous minerals is typical of oceanic sediments (Griffin et al., 1968; Gorbunova, 1970).

The formation of the upper sediments of Unit III, down to 519 meters, was accompanied by intensive calcite introduction, suggesting the existence of reefs around the Nauru Basin from the early Campanian to the Pleistocene, inclusive.

The history of palygorskite formation is obscure. There may have been several ways of its formation in sediments of Nauru Basin. Hydrothermal palygorskite growth is due to supply of magnesium solutions from a sill complex (Bonatti and Joensuu, 1968, 1969; Gorbunova, 1972; Lomova, 1975a, 1975b, 1979; Skornyakova et al., 1978), although the uneven and broken distribution of palygorskite in sediments of Unit III contradicts this (Table 5). The source of terrigenous palygorskite in Nauru Basin is obscure; also scanning electron micrographs do not show a terrigenous character.

Some students suggest authigenic palygorskite formation (Peterson et al., 1970; Zemmels and Cook, 1974; Couture, 1977). The occurrence of palygorskite mainly in red clays allows us to consider that the physical- chemical regime of red-clay formation is more favorable for the formation of palygorskite than for brown clays. At the same time, a high palygorskite content is found in Cretaceous brown clays in the northwestern Pacific Ocean (Leg 20; Matti et al., 1973). Thus, a conclusion about preferential conditions for the formation of palygorskite is unfounded. The assumption that during accumulation of red clays the material which easily released Mg was introduced to Nauru Basin is most probable. Such material was probably trioctahedral smectite, which could alter to dioctahedral smectite under oxidizing conditions. In this case, Fe^{+2} ox-

Table 8. Summary of identified minerals in volcaniclastic sediments from interbeds in basalts, Leg 61: <2 μm (1), 2-20 μm (2), >20 μm (3), bulk (4).

Sample (interval in cm)	Sub-bottom Depth (m)	Saponite				Hydromica				Chlorite				Analcime-Wairakite				Actinolite-Tremolite				Heulandite-Clinoptilolite				Talc			
		1	2	3	4	1	2	3	4	1	2	3	4	1	2	3	4	1	2	3	4	1	2	3	4	1	2	3	4
462-63-1, 25-27	579.5	X	X	X														X			X								
64-1, 40-42	585.5	X	X	X														X											
64-2, 35-38	587.0	X	X	X																									
64-3, 20-24	588.5	X	X	X											X	X													
65-1, 6-8	594.5	X	X	X											X	X													
462A-22-2, 88-90	590.0				X							X					X												
23-1, 0-2	597.0				X							X					X												
23-1, 4-6	597.0				X							X					X												
32-1, 105-107	656.5				X							X					X				X				X				
32-2, 71-73	657.5				X							X					X				X				X?				
40-1, 140-142	703.0				X																X				X?				
41-7, 109-111	712.0				X																X								
42-1, 54-56	720.5				X								X																
42-2, 93-95	722.0				X		X?					X					X												
42-2, 95-97	722.5				X								X																X?
43-1, 140-143	724.0				X							X					X												
43-2, 81-83	725.0				X							X					X												
43-2, 138-140	725.5				X							X					X												
79-6, 4-6	992.5	X	X	X										X	X	X													
80-1, 10-13	994.0				X								X																
80-1, 18-21	994.0				X			X					X																
80-1, 34-36	994.0				X								X																
80-2, 25-28	995.5	X	X	X											X	X										X?	X?		
80-2, 88-90	996.0				X								X																X
80-2, 97-102	996.0	X	X	X											X	X										X			

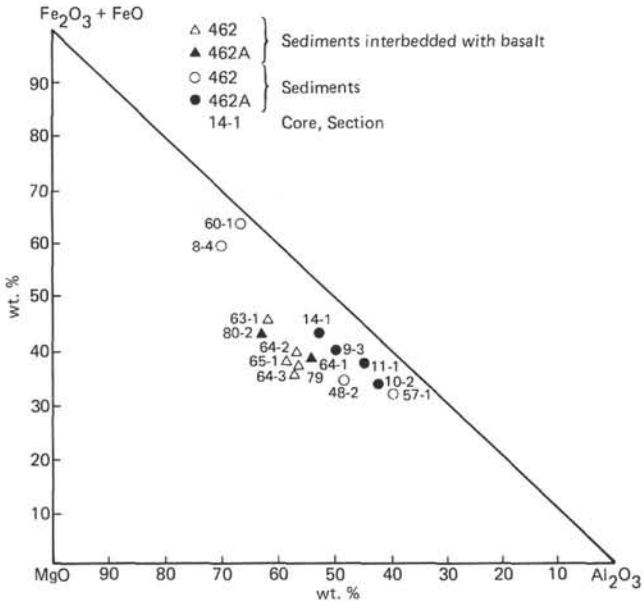

Figure 1. Triangular diagram of Fe_2O_3 + FeO–Al_2O_3–MgO for clay minerals from sediments and sediments interbedded with basalts at Site 462.

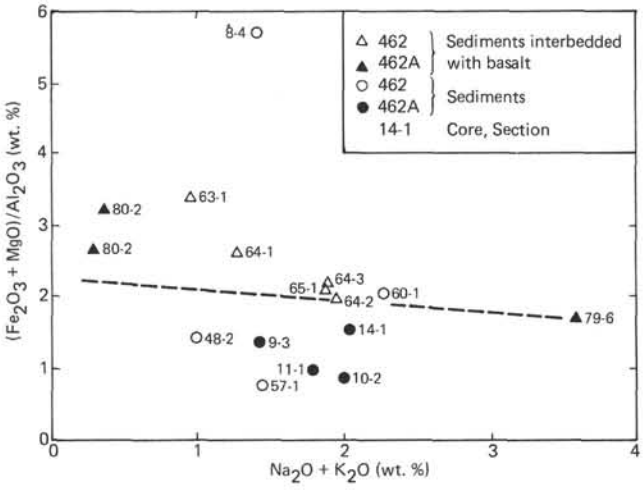

Figure 2. Variation of $(Fe_2O_3 + FeO + MgO)/Al_2O_3$ with $Na_2O + K_2O$ in clay minerals from sediments and sediments interbedded with basalt at Site 462.

idizes to Fe^{+3}, and Mg is released, which may be involved in palygorskite growth.

Growth of quartz and cristobalite-tridymite in the lower part of the sediments of Unit III, at the contact with basalt, irrespective of the type of rock, is connected with the final stages of sill volcanism in Nauru Basin. Sill volcanism also probably influenced the enrichment of the lower part of Unit III in manganese, iron, and potassium. Enrichment of rocks with SiO_2 and K is typical of the zone of solution degassing (Naboko, 1969).

An increase of Cr, Ni, Co, Sc, Pb, and Cu in sediments near the contact with basalt is observed in Hole 462A (Table 6) and is probably connected with the influence of sill volcanism on the material composition of sediments. Growth of metal-bearing sediments at the contact with basalt is widely described in the literature. The genesis of these sediments is questionable, although the majority of authors consider it to be exhalation-sedimentary, connected with the leaching of basalts heated (in fractures) by sea water, mainly in rift zones (Lisitsyn, 1978; and others). In Nauru Basin, metal-bearing sediments are related to intraplate magmatism.

Unit IV

Sediments of Unit IV, interbedded with basalts, consist of secondary minerals, mainly Fe-Mg-saponite. Primary sediments were composed of volcanic glass, probably tholeiitic.

Primary-glass alteration took place at 300 to 500°C and resulted in the formation of talc, actinolite-tremolite, analcime-wairakite, and chlorite. The temperature of formation of these minerals, accompanied by sea water-glassy-tholeiitic-basalt interaction, has been determined experimentally (Mottl et al., 1978; Kotov et al., 1978), and is described in this volume (Kurnosov et al.). Heulandite-clinoptilolite probably grew at 100 to 150°C (Senderov and Khitarov, 1970). Saponite was formed at lower temperatures. Secondary minerals were formed under reducing, alkalic conditions, similar to those of secondary minerals within basalts of Nauru Basin (Kurnosov et al., this volume).

Besides temperature, the alteration of glass in sediments was influenced by solutions introduced to volcanic sediments from cooling sills. The nature of solutions in sills is considered in this volume (Kurnosov et al.). Sub-vertical veinlets of zeolites discovered by the participants of Leg 61 in sediments of Unit IV testify to this. Saponites from sediments are probably not only the product of *in situ* glass decomposition; they may also grow from solutions introduced along open fractures in sills. Saponites from volcaniclastic sediments of Unit IV and from veins within basalts are similar in chemical composition and content of minor elements (Tables 3, and 7; Kurnosov et al., this volume).

CONCLUSIONS

Mineralogical analysis of sediments from Nauru Basin allows us to consider that a complex of calcareous and siliceous sediments, consisting of terrigenous minerals which did not undergo notable diagenetic changes, was formed in Eocene–Pleistocene time. The terrigenous mineral complex reflects common paleogeographic conditions of sedimentation—a regime of oceanic pelagic sedimentation, reef knolls surrounding Nauru Basin, some island alkali volcanism, and suspension flows, introduction of homogeneous clay material to Nauru Basin, and long relative stability of oceanic currents transporting clay minerals to the basin.

In Cretaceous time, volcaniclastic sediments which accumulated in Nauru Basin differ in mineralogical composition both from terrigenous Eocene–Pleistocene sediments and among themselves. Their accumulation suggests active volcanism—probably under-water tholeiitic volcanism in middle Cretaceous time, and sub-

aerial alkali volcanism on islands surrounding Nauru Basin in Cenomanian–Maestrichtian time. Alteration of volcaniclastic sediments overlying the sill complex and interbedded with it took place under different conditions and ended in the formation of unlike mineralogical associations.

Alteration of middle Cretaceous volcaniclastic sediments within the sill complex took place under conditions close to those of vein mineral formation within basalts of Nauru Basin: 500°C and lower, a semi-closed system with difficult water exchange, and an alkalic, reducing regime. As a result, high- and middle-temperature minerals have grown: talc, actinolite–tremolite, analcime–wairakite, chlorite, heulandite–clinoptilolite, and trioctahedral smectite (Fe–Mg-saponite). This association is akin to the complex of secondary minerals in basalts.

Upper Cretaceous volcaniclastic sediments overlying the sill complex were altered by low-temperature interaction with sea water, in an open system. Thus, dioctahedral smectite (Fe-montmorillonite), often clinoptilolite, and sometimes palygorskite are the main secondary minerals.

Comparison of conditions of formation of smectites from volcaniclastic sediments and from basalts (Kurnosov et al., this volume) shows that a semi-closed system (autoclave) and reducing regime (volcaniclastic sediments between sills, groundmass basalt, and veins in basalts) are necessary for the formation of trioctahedral smectites. Under experimental conditions similar to natural ones, trioctahedral smectite is also the main product of tholeiitic basalt alteration (Mottl et al., 1978; Kotov et al., 1978).

Dioctahedral smectites grow under oxidizing conditions in open systems (volcaniclastic sediments overlying the sill complex, volcaniclastic layers in terrigenous Eocene–Pleistocene sediments, and the upper part of the sill complex with celadonite–glauconite; see Kurnosov et al., this volume). The reason for palygorskite concentration in the red clays is obscure.

The proximity of the sill complex manifested itself in silicification (quartz, cristobalite–tridymite) of about 20 meters of sediments overlying basalt, and in an increase in Mn, Fe, K, Cr, Ni, Co, Sc, Pb, and Cu in sediments near the contact with basalt.

ACKNOWLEDGMENTS

We thank Dr. S. A. Shcheka, Dr. N. O. Murdmaa, Dr. H. Okada, and Dr. N. V. Kotov for comments and criticism. We also thank N. V. Gruda, I. V. Kholodkevich, T. V. Sverkunova, L. I. Kovbas, T. L. Plakhova, and N. G. Engovatova for assistance during various parts of the study.

REFERENCES

Bonatti, E., and Joensuu, O., 1968. Palygorskite from Atlantic deep-sea sediments. *Am. Mineral.*, 53:975–983.

_____, 1969. Palygorskite from the deep-sea: a reply. *Am. Mineral.*, 54:568.

Butuzova, G. Yu., Dritz, V. A., Lisitsina, N. A., et al., 1979. Dynamics of clay minerals formation in ore-bearing sediments of the Atlantis-II basin. *Lithol. Mineral. Res.*, 1:30–42.

Couture, R. A., 1977. Composition and origin of palygorskite-rich and montmorillonite-rich zeolite-containing sediments from the Pacific Ocean. *Chem. Geol.* 19:2.

Dritz, V. A., and Sakharov, B. A., 1976. *X-Ray Structural Analysis of Mixed-Layer Minerals:* Moscow (Nauka).

Griffin, J., Windom, H., and Goldberg, E., 1968. The distribution of clay minerals in the World Ocean. *Deep-Sea Res.*, 15:433–459.

Gorbunova, Z. N., 1970. Clay and other highly dispersed minerals in Pacific sediments. *The Pacific Ocean*, (Vol. 1); Moscow (Nauka).

_____, 1972. Palygorskites in sediments from cores of deep-water drilling in the Pacific Ocean. *Trans. Acad. Sci. U.S.S.R.*, 207:430–432.

Kossovskaya, A. G., and Shutov, V. D., 1975. *Minerals—Indicators of Geotectonic Types of the Regional Epigenesis and Its Conjugation with Metamorphism on Continents and in Oceans. Crystallochemistry of Minerals and Geological Problems:* Moscow (Nauka), pp. 19–34.

Kotov, N. V., Kurnosov, V. B., and Kholodkevich, I. V., 1978. Modelling of natural processes of volcanic rock transformation in pure and model sea water at higher P–T parameters. *Lithol. Mineral. Res.*, 4:78–89.

Kurnosov, V. B., Tseitlin, N. V., and Narnov, G. A., 1980. Clay minerals: paleogeographic and diagenetic aspects. *In* Scientific Party, *Init. Repts. DSDP*, 56, 57, Pt. 2: Washington (U.S. Govt. Printing Office), 979–1004.

Lisitsyn, A. P., 1978. *Processes of Oceanic Sedimentation. Lithology and Geochemistry:* Moscow (Nauka).

Lomova, O. S., 1975a. Abyssal palygorskite clays in the East Atlantic and their genetic relations with alkaline volcanicity (according to the data of the 2nd and 14th *Glomar Challenger* voyages). *Lithol. Mineral Res.*, 4:10–27.

_____, 1975b. *Abyssal palygorskite clays of the East Atlantic (Legs 2, 14,* "Glomar Challenger"). *Crystallochemistry of Minerals and Geological Problems:* Moscow (Nauka), pp. 105–115.

_____, 1979. Palygorskites and sepiolites as indicators of geological environments. *Trans. Acad. Sci. U.S.S.R.*, 336:117–123.

Matti, J. C., Zemmels, I., and Cook, H. E., 1973. X-ray mineralogy of sediment from the western Pacific, Leg 20, DSDP. *In* Heezen, B. C., MacGregor, I. D., et al., *Init. Repts. DSDP*, 20: Washington (U.S. Govt. Printing Office), 323–334.

_____, 1974. X-ray mineralogy data, northwestern part of the Indian Ocean. *In* von der Borsch, C. C., Slater, J. G., et al., *Init. Repts. DSDP*, 22: Washington (U.S. Govt. Printing Office), 693–710.

Mering, J., 1975. Smectites. Soil components. *Inorgan. Compon.*, 2: 97–119.

Mottl, M. J., and Holland, H. D., 1978. Chemical exchange during hydrothermal alteration of basalt by seawater. I. Experimental results for major and minor components of seawater. *Geochim. Cosmochim. Acta*, 42:1103–1115.

Naboko, S. I., 1969. *Conditions of Formation and Peculiarities of Recent Hydrothermal Metasomatic Formation of Kurile–Kamchatka Volcanic Arc. Young Hydrothermally Altered Rocks and Minerals of Kamchatka and Kurile Islands:* Moscow (Nauka), pp. 3–8.

Peterson, M. N. A., Edgar, N. T., von der Borch, C. C., et al., 1970. Cruise leg summary and discussion. *In* Peterson, M. N. A., Edgar, N. T., et al., *Init. Repts. DSDP*, 2: Washington (U.S. Govt. Printing Office), 9–249.

Senderov, E. E., and Khitarov, N. I., 1970. *Zeolites, Their Synthesis and Conditions of Formation in Nature:* Moscow (Nauka).

Skornyakova, N. S., Kurnosov, V. B., Svalnov, V. N., et al., 1978. Sepiolites and palygorskites in the Indian Ocean. *Lithol. Mineral Res.*, 6:29–45.

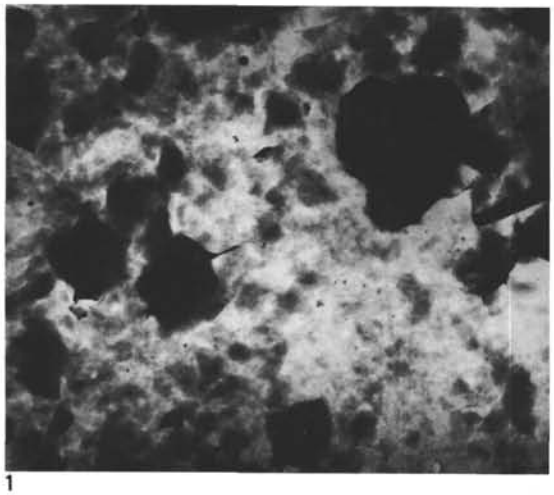

1

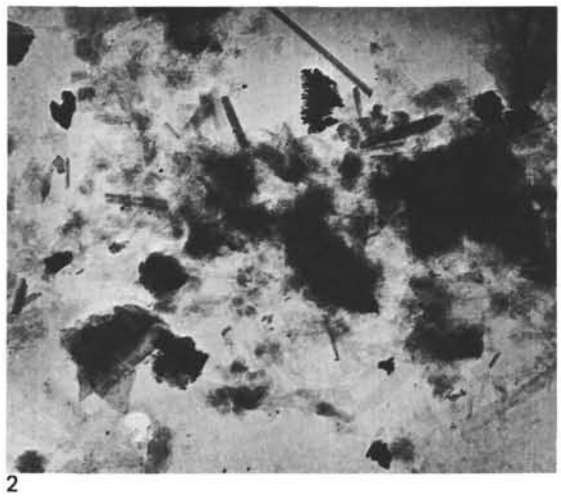

2

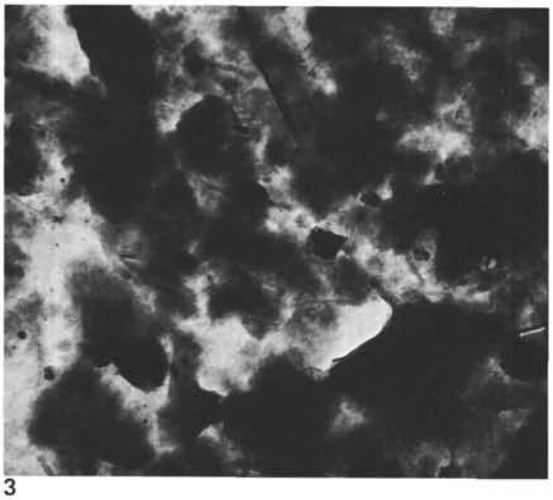

3

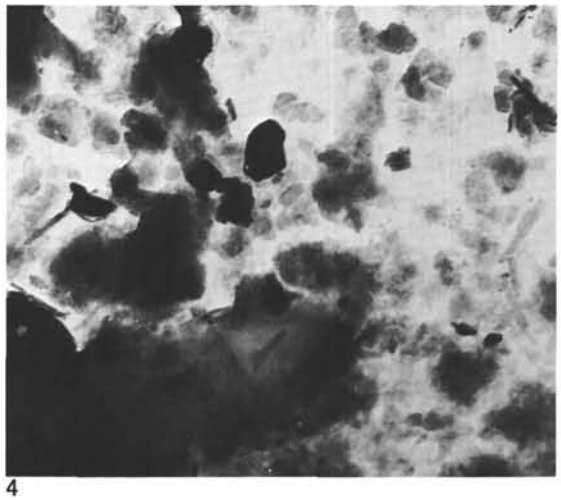

4

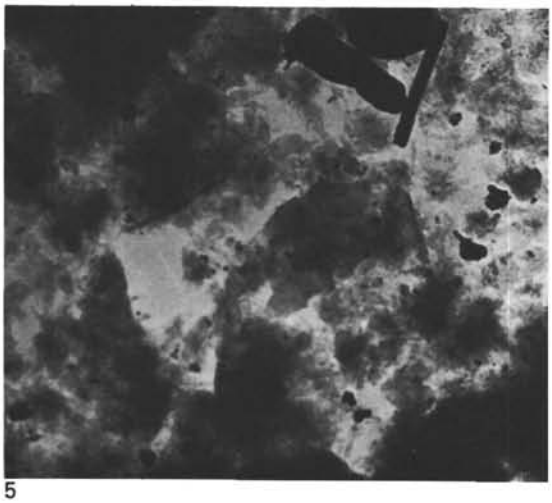

5

6

Plate 1. Electron micrographs of clay minerals from sediments and sediments interbedded with basalts, Leg 61.

Figures 1–3. Fe-montmorillonite. 1. Sample 462-48-2, 75–77 cm, ×10,000 2. Sample 462A-9-3, 58–61 cm, ×20,000 3. Sample 462A-11-1, 60–64 cm, ×20,000

Figure 4. Fe–Mg-saponite, ×40,000. Sample 462A-80-1, 34–36 cm.

Figure 5. Mixed-layer hydromica–montmorillonite, ×40,000. Sample 462-18-3, 74–78 cm.

Figure 6. Palygorskite, ×5000. Sample 462A-10-2, 109–116 cm.

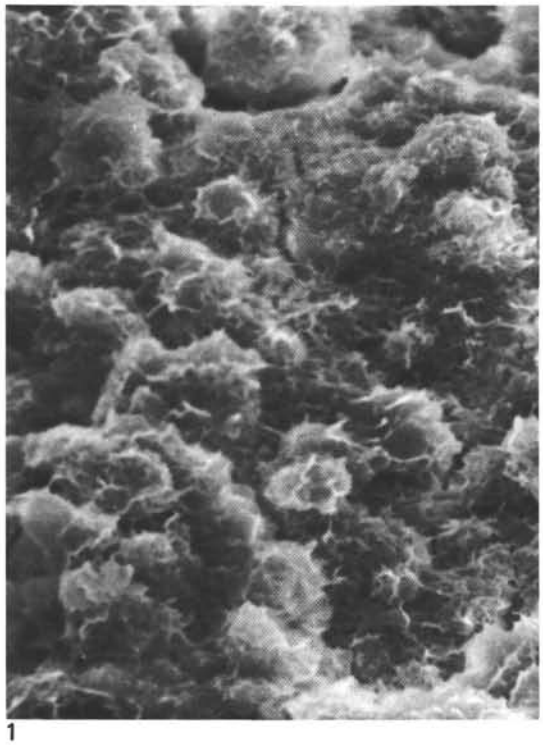

1

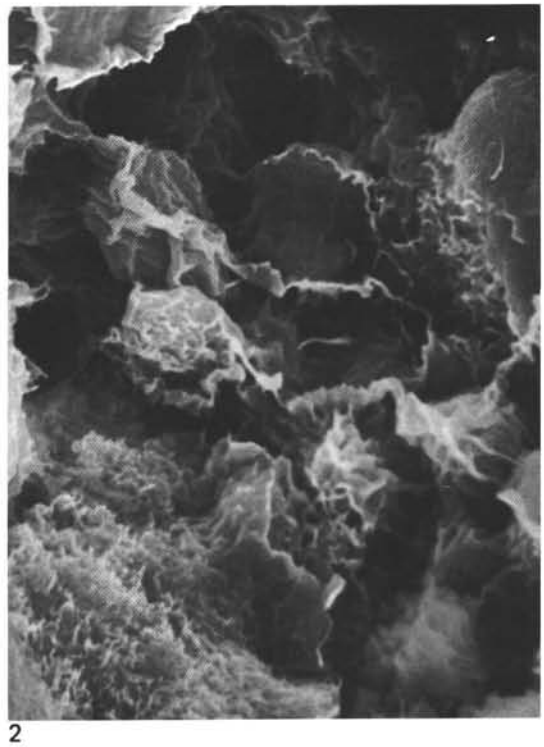

2

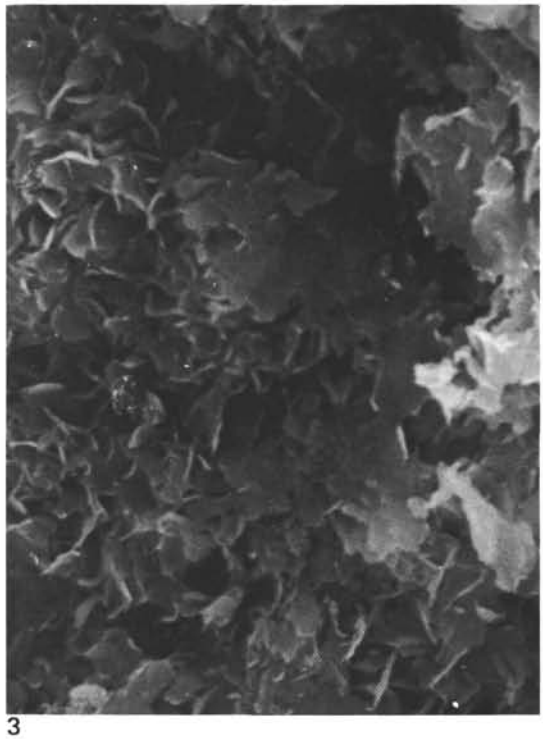

3

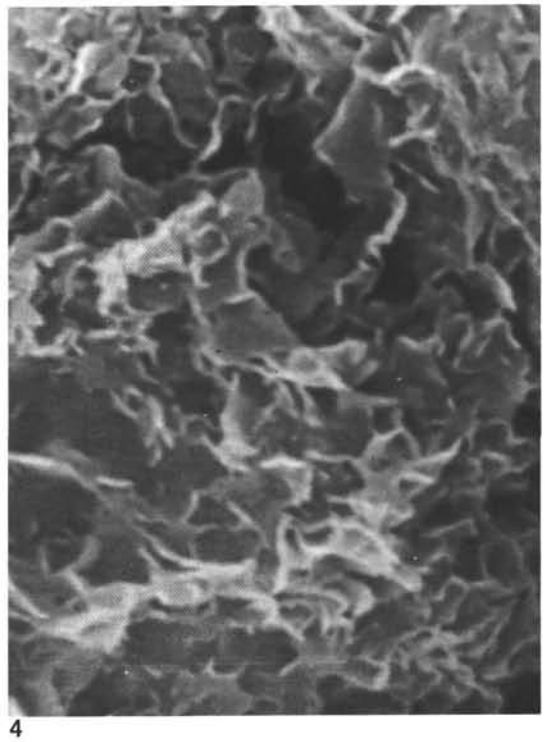

4

Plate 2. Scanning electron micrographs of smectites from sediments and sediments interbedded with basalts, Leg 61.

Figures 1, 2. Fe-montmorillinite. 1. Sample 462-48-2, 75–77 cm, ×1000. 2. Sample 462-57,CC, ×2000.
Figures 3, 4. Fe–Mg-saponites. 3. Sample 462-65-1, 6–8 cm, ×3000. 4. Sample 462A-80-1, 34–36 cm, ×10,000.

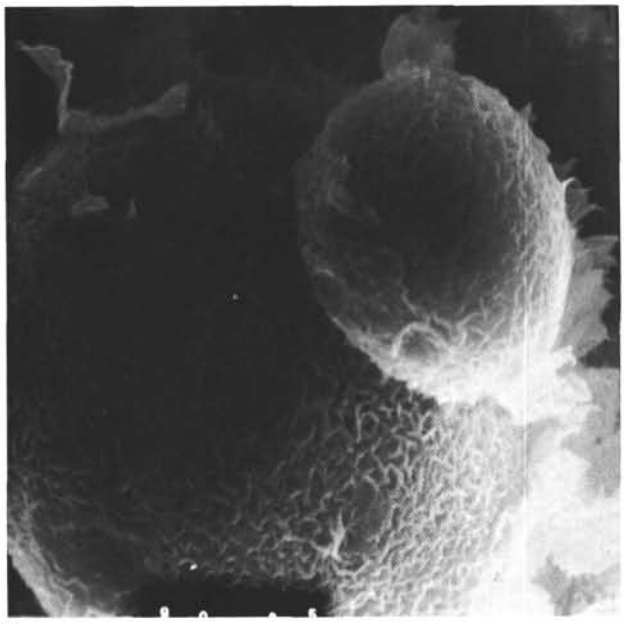

1

Plate 3. Scanning electron micrographs of secondary minerals from volcaniclastic sediments, Leg 61.

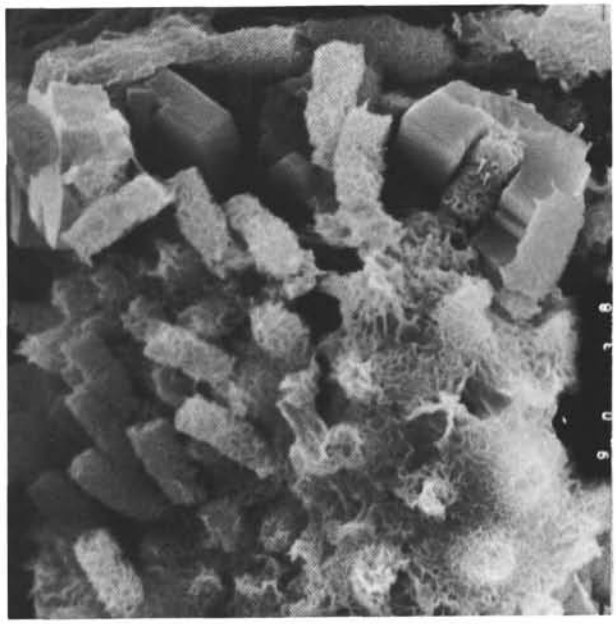

2

Figure 1. Fe-montmorillonite, ×2600. Sample 462-48-2, 75–77 cm.
Figure 2. Fe-montmorillonite and zeolite, ×2000. Sample 462-57, CC.

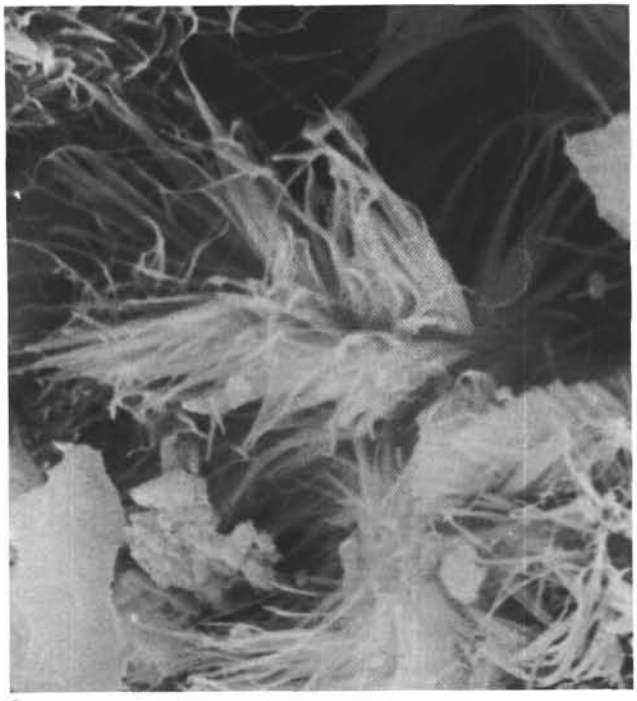

1

Plate 4. Scanning electron micrographs of palygorskite, Leg 61.

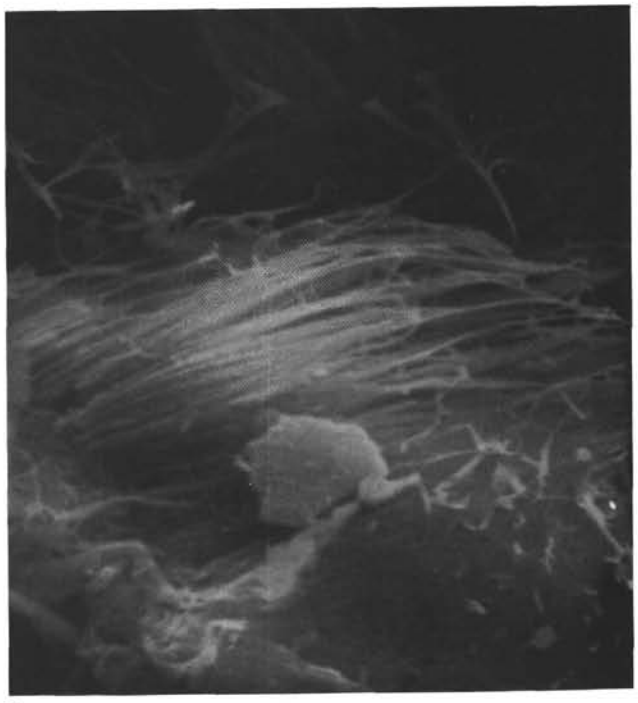

2

Figure 1. Sample 462-50-2, 138–141 cm, ×3000.
Figure 2. Sample 462-50-2, 138–141 cm, ×4000.

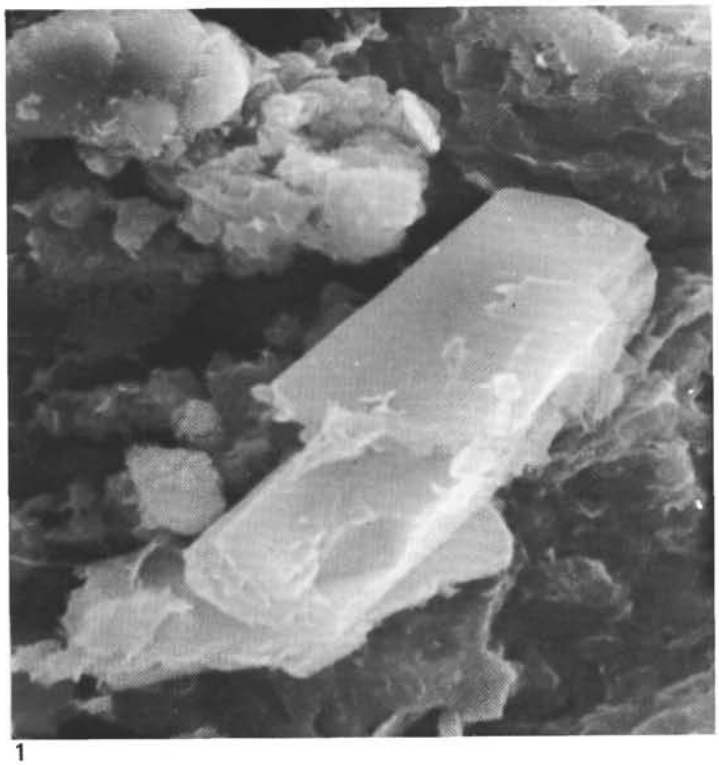

1

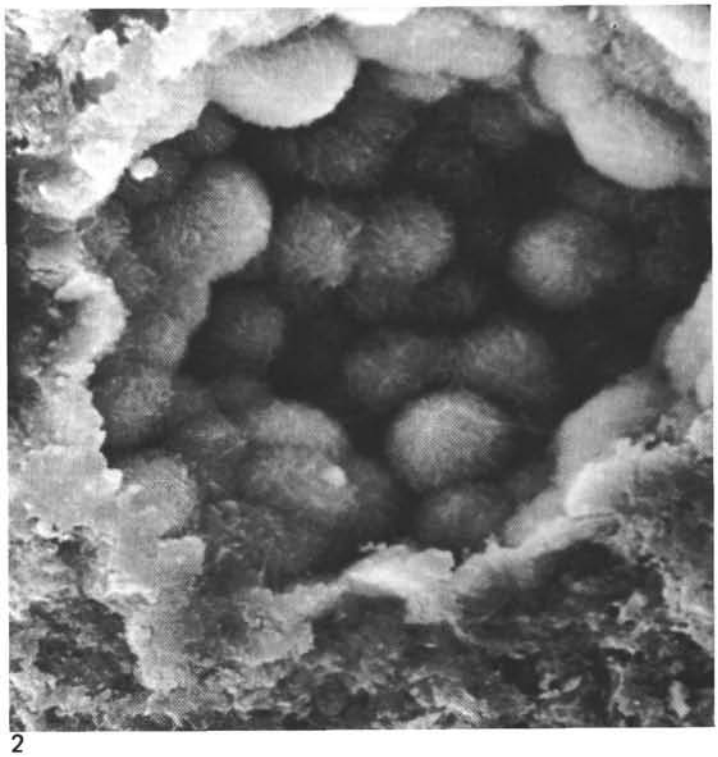

2

Plate 5. Scanning electron micrographs of secondary minerals, Leg 61.

Figure 1. Clinoptilolite and Fe-montmorillonite, ×3000. Sample 462A-11-1, 60–62 cm.

Figure 2. Cristobalite–tridymite (opal-CT), ×900. Sample 462-59-1, 0–5 cm.

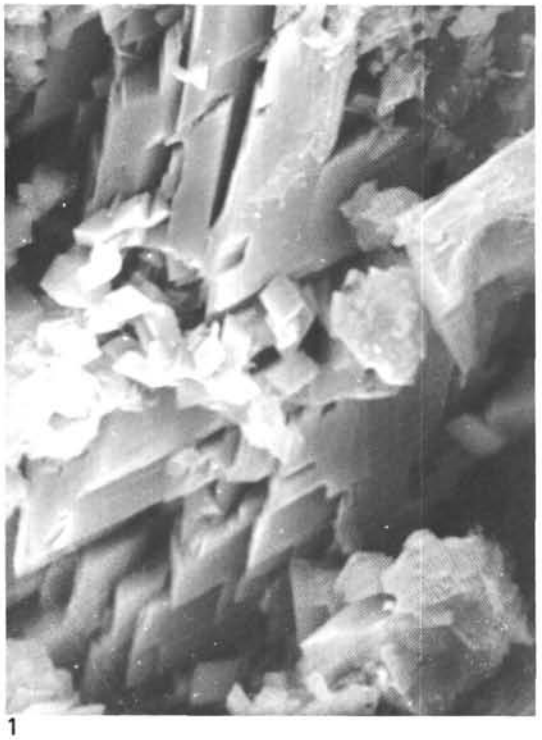

1

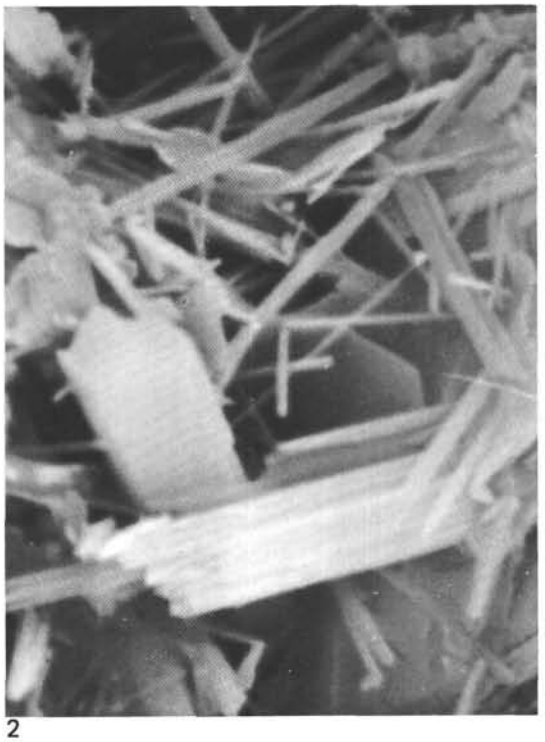

2

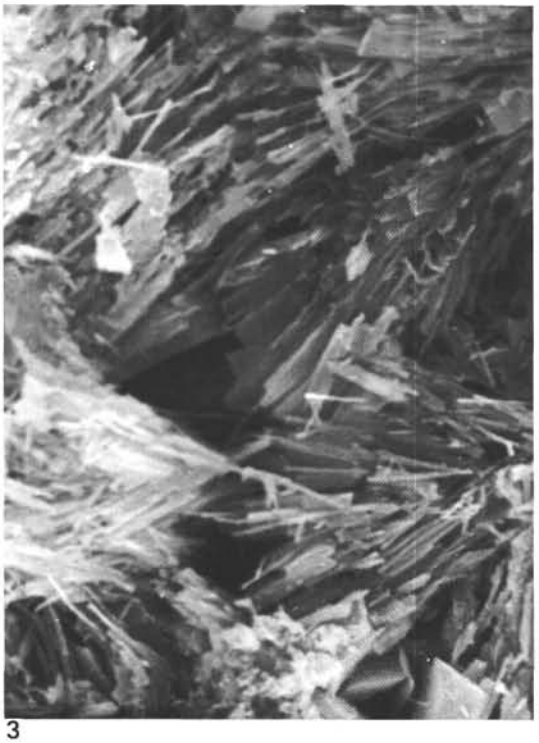

3

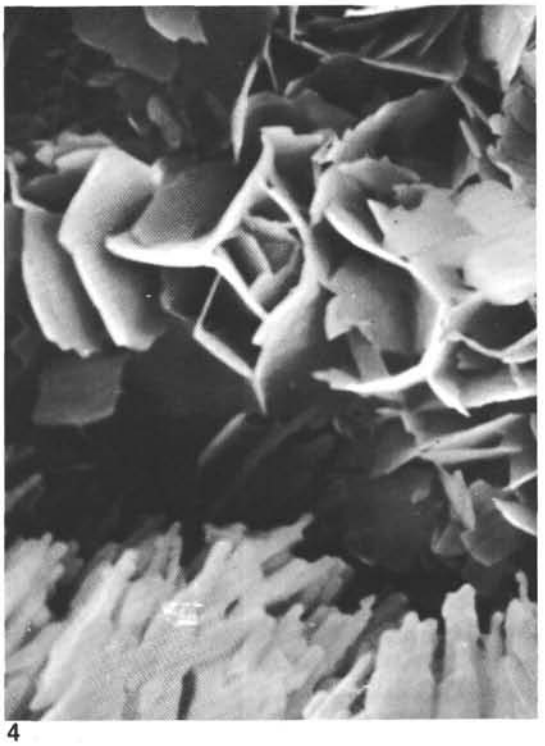

4

Plate 6. Scanning electron micrographs of secondary minerals, Leg 61.

Figure 1. Analcime-wairakite, ×1000. Sample 462-65-1, 6–8 cm.

Figure 2. Saponite, ×9000. Sample 462A-32-1, 105–107 cm.
Figure 3. Zeolite, ×4500. Sample 462A-42-2, 95–97 cm.
Figure 4. Smectite (center) and zeolite (below). Sample 462A-43-2, 81–83 cm, ×3000.

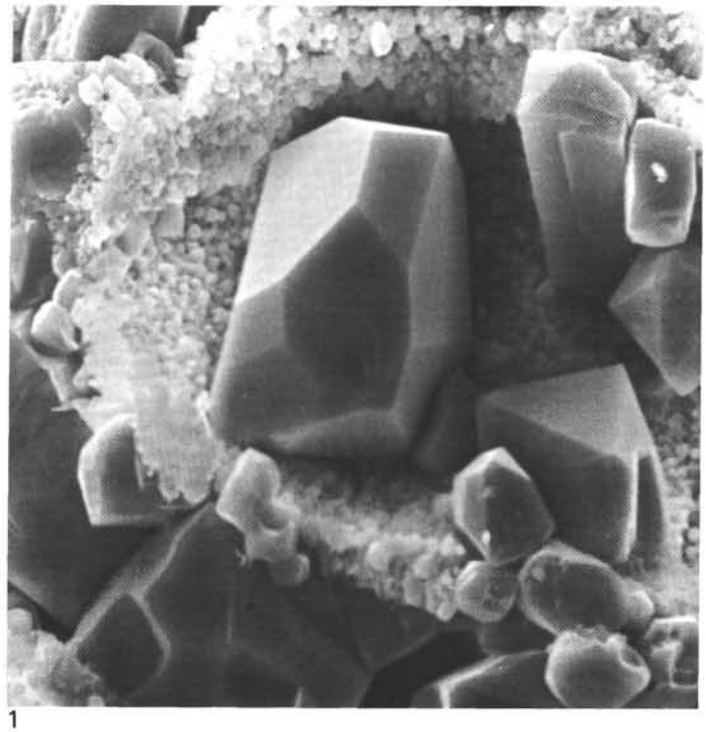

1

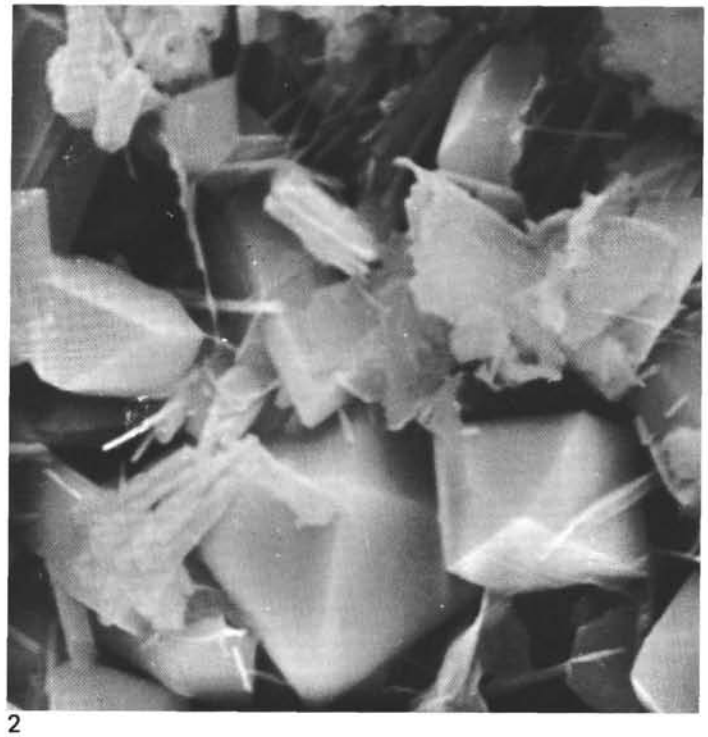

2

Plate 7. Scanning electron micrographs of secondary minerals, Leg 61.

Figure 1. Clinoptilolite. Sample 462A-7-1, 46–51 cm, ×1000.
Figure 2. Clinoptilolite and needle-like zeolites(?). Sample 462A-42-2, 95–97 cm, ×6000.